The Astronomical Journal, 146:146 (9pp), 2013 December doi:10.1088/0004-6256/146/6/146

ABSOLUTE PROPERTIES OF THE ECLIPSING BINARY VV CORVI

Francis C. Fekel[1,3], Gregory W. Henry[1], and James R. Sowell[2]
[1] Center of Excellence in Information Systems, Tennessee State University, 3500 John A. Merritt Boulevard, Box 9501, Nashville, TN 37209, USA; fekel@evans.tsuniv.edu, gregory.w.henry@gmail.com
[2] School of Physics, Georgia Institute of Technology, Atlanta, GA 30332, USA; jim.sowell@physics.gatech.edu
Received 2013 July 17; accepted 2013 September 25; published 2013 October 29

ABSTRACT

We have obtained red-wavelength spectroscopy and Johnson *B* and *V* differential photoelectric photometry of the eclipsing binary VV Crv = HR 4821. The system is the secondary of the common proper motion double star ADS 8627, which has a separation of 5.″2. VV Crv has an orbital period of 3.144536 days and a low but non-zero eccentricity of 0.085. With the Wilson–Devinney program we have determined a simultaneous solution of our spectroscopic and photometric observations. Those orbital elements produce masses of $M_1 = 1.978 \pm 0.010\ M_\odot$ and $M_2 = 1.513 \pm 0.008\ M_\odot$, and radii of $R_1 = 3.375 \pm 0.010\ R_\odot$ and $R_2 = 1.650 \pm 0.008\ R_\odot$ for the primary and secondary, respectively. The effective temperatures of the two components are 6500 K (fixed) and 6638 K, so the star we call the primary is the more massive but cooler and larger component. A comparison with evolutionary tracks indicates that the components are metal rich with [Fe/H] = 0.3, and the system has an age of 1.2 Gyr. The primary is near the end of its main-sequence lifetime and is rotating significantly faster than its pseudosynchronous velocity. The secondary is still well ensconced on the main sequence and is rotating more slowly than its pseudosynchronous rate.

Key words: binaries: close – binaries: eclipsing – binaries: spectroscopic – stars: individual (VV Crv)

Online-only material: color figures, machine-readable and VO tables

1. INTRODUCTION

The bright star HR 4821 = HD 110317 = VV Crv ($\alpha = 12^h41^m15^s.95$, $\delta = -13°00'50''.0$ (2000)) is the slightly fainter component of the common proper motion pair ADS 8627, which has a separation of 5.″2 (Mason et al. 2007). Tokovinin et al. (2006) estimated an orbital period of ∼4500 yr for the A–B pair. Another, much fainter, visual companion, component C at a separation of 58.″5, is also believed to be a member of the system (Tokovinin et al. 2006). The visual components A and B differ in *V* by just 0.1 mag (Sinachopoulos 1993) and also have similar mid-F spectral types (Cowley & Bidelman 1979; Abt 1981, 2009). From radial velocities obtained at Simeis Observatory, Shajn & Albitzky (1932) found both the A and B components to be spectroscopic binaries. Using observations acquired at Mount Wilson Observatory, Sanford & Karr (1942) determined orbital periods of 44.41 days and 1.46 days for A and B, respectively. Collecting new radial velocities of HR 4821, Massarotti et al. (2008) also computed an orbit for it with the 1.46 day period. *Hipparcos* photometry of the combined A–B system, presented in the Variability Annex of the *Hipparcos* and *Tycho* catalogs (Perryman & ESA 1997), shows that one component of the A–B pair is an eclipsing binary with an orbital period of 3.145 days. Because of this variability, Kazarovets et al. (1999) assigned the system the variable star designation VV Crv.

In 2002 we began a program to enhance the spectroscopic orbit precision of potential interferometric binaries (Fekel & Tomkin 2004). Observations to produce a combined spectroscopic–astrometric orbit will provide accurate masses, a precise orbital parallax, and other basic quantities that can be compared with theoretical results. In the past, some interferometric binary studies (e.g., Boden et al. 2005) have included new, high-quality radial velocities; however, at times radial velocities simply have been taken from the literature (e.g., Armstrong et al. 1992). An additional objective of this binary star program is the spectroscopic detection of previously unseen secondary components, turning single-lined binaries into much more useful double-lined binaries. For example, the binary mass ratio distribution is an important diagnostic for assessing models of binary formation (e.g., Halbwachs et al. 2003). Finally, obtaining radial velocities of known spectroscopic binaries at a substantially different epoch can result in the discovery of a third component, increasing the known multiplicity of systems (Mayor & Mazeh 1987). Such a knowledge is needed for the statistics of multiple systems and an understanding of their origin (Tokovinin 2008). Currently, complimentary interferometric observations are being obtained of 10 of our spectroscopic binary systems.

As part of this program, we initially obtained spectroscopic observations of component A, HR 4822, the brighter star of the relatively close visual pair. However, after collecting spectra for several seasons we decided to observe component B, HR 4821, as well. Upon discovering that the *Hipparcos* team had found one component of the visual system to be an eclipsing binary, we also acquired photometric observations of the A–B system.

Our spectroscopic and photometric observations clearly identify HR 4821, component B of the close common proper motion pair, as the eclipsing binary VV Crv, and we confirm the 3.145 day period found in the *Hipparcos* photometry. In addition we determine the basic properties of VV Crv and discuss its evolutionary status. Component A, HR 4822, which our spectroscopic observations show to be a triple system, will be the subject of a separate paper once at least one cycle (∼9 yr) of its long-period orbit has been covered. Thus, if component C is indeed a physical member, the entire system consists of at least six stars.

2. SPECTROSCOPIC OBSERVATIONS AND REDUCTIONS

From 2010 March through 2012 June we acquired 35 usable spectrograms with the Tennessee State University 2 m automatic spectroscopic telescope (AST) and a fiber-fed echelle spectrograph (Eaton & Williamson 2007), which is situated at Fairborn

[3] Visiting Astronomer, Kitt Peak National Observatory, National Optical Astronomy Observatory, operated by the Association of Universities for Research in Astronomy, Inc., under cooperative agreement with the National Science Foundation.

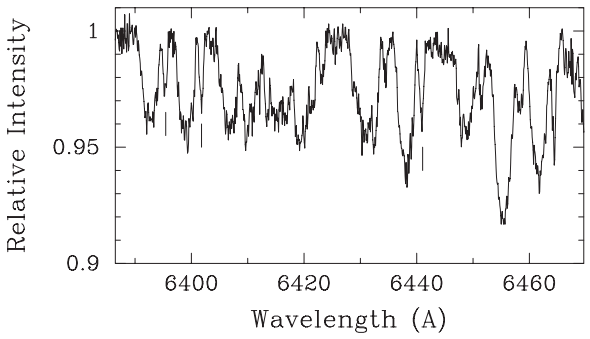

Figure 1. Spectrum of VV Crv in the 6430 Å region. Lines of the primary are blueshifted. Three lines of the redshifted secondary are indicated by tick marks.

Observatory in southeastern Arizona. For the first 16 months of observation, the detector was a 2048 × 4096 SITe ST-002A CCD. Those echelle spectrograms have 21 orders, span the wavelength range 4920–7100 Å (Eaton & Williamson 2007), and have a resolution of 0.24 Å. In the summer of 2011 the SITe CCD detector and dewar were retired. The new AST detector is a Fairchild 486 CCD, having 4096 × 4096 15 μm pixels, that is housed in a new dewar. See Fekel et al. (2013) for additional information about the 2 m AST upgrades. The spectrograms that were obtained with this new detector have 48 orders covering the wavelength range 3800–8260 Å. The spectral resolution with the Fairchild CCD is the same, 0.24 Å, as that with the SITe CCD. Depending on weather conditions and the CCD used, we acquired spectra that have signal-to-noise ratios (S/Ns) ranging from 70 to 140 at 6000 Å.

In 2012 May we also obtained two observations of VV Crv with the Kitt Peak National Observatory (KPNO) coudé feed telescope and coudé spectrograph. The detector was a CCD that was made by Semiconductor Technology Associates and designated STA2. It consists of a 2600 × 4000 array of 12 μm pixels. The spectrograms are centered at 6430 Å, cover a wavelength range of 336 Å, and have a resolution of 0.21 Å. Both spectra have S/Ns of about 150.

Fekel et al. (2009) have provided a general description of the velocity measurement for the Fairborn Observatory echelle spectra. Given the mid-F spectral type of VV Crv, we chose to measure the lines included in our solar-type star line list. Because the components have moderately large rotational velocities (Figure 1), we have fitted the lines with rotationally broadened profiles (Fekel & Griffin 2011) rather than Gaussians.

The Fairborn AST velocities are on an absolute scale. When compared to the results of Scarfe (2010), our unpublished measurements of several IAU solar-type velocity standards show that the Fairborn Observatory velocities from the SITe CCD have a small zero-point offset of −0.3 km s^{-1}. Thus, we have added 0.3 km s^{-1} to each of those Fairborn velocities. Similarly, we have determined that the velocities that have been obtained with the Fairchild CCD have a zero-point offset of −0.6 km s^{-1} relative to those of Scarfe (2010). Thus, 0.6 km s^{-1} has been added to each of those velocities.

For the Fairborn spectra, Table 1 provides the heliocentric Julian dates of mid-observation and the corresponding velocities of the primary and secondary components. Also listed is the fractional phase for each observation, which is computed from a time of periastron, and the residuals to the orbit from the spectroscopic solution discussed in Section 4. Given the very small number of KPNO spectra, we did not include velocity measurements of them in our solution. We have also reanalyzed the velocities of Massarotti et al. (2008), which are provided in the SB9 catalog (Pourbaix et al. 2004), and so in Table 2 we list them in the same manner as our Fairborn observations.

Table 1
Fairborn Observatory Radial Velocity Observations[a]

Helio. Julian Date (HJD − 2400000)	Phase	V_1 (km s^{-1})	$(O-C)_1$ (km s^{-1})	V_2 (km s^{-1})	$(O-C)_2$ (km s^{-1})
55260.902	0.959	−63.3	0.1	60.5	0.9
55274.884	0.405	54.4	0.8	−94.5	−0.3
55280.857	0.305	78.8	−1.4	−127.5	1.7
55599.974	0.789	−105.4	0.7	115.0	−0.8
55607.944	0.324	79.5	2.3	−126.0	−0.7
55615.950	0.870	−103.3	−1.7	109.6	−0.3
55631.829	0.919	−83.6	0.7	87.1	−0.1
55640.879	0.797	−103.9	3.0	117.7	0.8
55671.901	0.663	−67.7	0.6	66.4	0.2
55687.853	0.736	−96.2	−0.9	100.8	−0.9
55703.758	0.794	−105.4	1.2	115.8	−0.7
55726.753	0.107	36.8	0.9	−73.0	−2.1
55739.694	0.222	80.3	0.5	−129.5	−0.8
55889.007	0.706	−88.8	−3.1	88.3	−0.6
55924.937	0.132	50.8	0.9	−90.2	−0.8
55940.957	0.227	79.5	−1.0	−128.2	1.4
55981.925	0.255	80.8	−2.1	−131.8	1.0
56003.754	0.197	73.4	−1.3	−122.7	−0.7
56008.778	0.795	−103.3	3.4	116.6	0.0
56013.897	0.423	49.8	3.1	−85.6	−0.4
56014.754	0.696	−84.6	−2.8	83.8	0.0
56016.916	0.383	63.2	1.8	−103.8	0.8
56019.865	0.321	80.6	3.0	−126.7	−0.8
56021.838	0.948	−69.0	0.5	68.7	1.1
56022.694	0.221	76.3	−3.2	−128.8	−0.4
56025.890	0.237	81.4	−0.3	−130.8	0.4
56027.891	0.873	−98.3	2.4	108.6	−0.1
56030.693	0.764	−101.5	0.8	110.5	−0.3
56033.725	0.729	−93.6	−0.4	99.2	0.4
56035.768	0.378	64.3	1.3	−106.5	0.1
56038.925	0.382	63.5	1.8	−105.8	−0.9
56039.825	0.669	−72.3	−1.5	70.3	0.9
56041.825	0.305	80.3	0.1	−128.6	0.7
56054.678	0.392	58.6	0.2	−101.4	−0.8
56061.710	0.628	−53.4	−1.0	44.9	−0.3

Note. [a] Phases and $(O-C)$ residuals are computed with the spectroscopic values presented in Table 4.

3. PHOTOMETRIC OBSERVATIONS AND REDUCTIONS

We acquired our photometric observations of VV Crv on 76 nights between 2012 March 5 and June 21 with the T3 0.4 m Automatic Photoelectric Telescope (APT) at Fairborn Observatory. T3 is one of eight telescopes operated by Tennessee State University at Fairborn for automated photometry, spectroscopy, and imaging (Henry 1995, 1999; Eaton et al. 2003; Eaton & Williamson 2007). T3's precision photometer is based around an EMI 9924B photomultiplier tube (PMT) that measures photon count rates successively through Johnson B and V filters. To maximize the stability of the photometer, the PMT, voltage divider, pre-amplifier electronics, and photometric filters are all mounted within the temperature- and humidity-controlled body of the photometer. The precision of a single observation on a good night is usually in the range of ∼0.003–0.005 mag (e.g., Johnson et al. 2011, Table 20), depending primarily on the brightness of the target and the airmass of the observation.

Table 2
Reanalyzed Massarotti et al. (2008) Radial Velocity Observations[a]

Helio. Julian Date (HJD − 2400000)	Phase	V_1 (km s^{-1})	$(O-C)_1$ (km s^{-1})	V_2 (km s^{-1})	$(O-C)_2$ (km s^{-1})
53002.8712	0.885	−97.41	−1.16	104.91	−1.14
53038.8136	0.315	75.69	−3.17	−129.08	−1.59
53088.6984	0.178	48.42[b]	−18.03	−123.97[b]	−13.03
53372.9375	0.569	−24.45	−4.69	−26.54[b]	−30.57
53419.8027	0.473	26.52	−1.13	−56.05	3.14
53460.7268	0.487	29.44	8.41	−52.58	−2.21
53868.7042	0.227	79.90	1.21	−129.64	−2.37
54108.0568	0.344	71.75	−1.83	−120.34	0.12
54131.0176	0.645	−55.83	1.45	54.78	0.71
54159.9247	0.838	−106.32	−1.64	125.72	8.43
54159.9621	0.850	−103.17	0.27	112.47	−3.16
54194.7780	0.922	−81.32	1.42	89.95	1.91
54194.7852	0.924	−79.78	1.94	87.27	0.60
54225.7299	0.765	−100.14	−0.55	112.36	1.86
54246.6913	0.431	47.65	1.88	−84.15	−0.79
54249.6953	0.386	61.37	−0.66	−104.99	0.05
54250.6482	0.689	−77.01	−0.86	76.95	−2.29
54252.6485	0.325	76.82	−0.41	−124.16	1.16
54253.7309	0.669	−66.91	1.08	69.12	0.76
54255.6489	0.279	81.92	0.00	−131.22	0.35
54256.6503	0.598	−37.49	−3.29	13.61	−9.68
54277.6449	0.274	84.02	2.00	−133.14	−1.43
54278.6905	0.607	−22.77[b]	15.90	8.86[b]	−20.39
54281.6769	0.556	−13.04	0.28	0.48	5.04
54282.6507	0.866	−100.13	0.64	107.72	−4.36
54283.6445	0.182	66.87	−0.79	−114.32	−1.76
54284.6380	0.498	20.88	5.17	−41.45	1.82
54285.6303	0.813	−102.96	2.36	110.41	−7.74
54286.6508	0.138	50.09	0.54	−92.75	−4.34

Notes.
[a] Phases and $(O-C)$ residuals are computed with the spectroscopic values presented in Table 4.
[b] Velocity given zero weight.

Since all our targets are bright (see below), we used a 1.2 mag neutral density filter for all observations to attenuate the count rates and minimize all deadtime corrections. All integration times were 15 s. Finally, we used a 55″ focal-plane diaphragm for all measurements. This diaphragm admits the light from the close visual pair A and B as well as their spectroscopic and unseen companions. However, component C, which is at a separation of the 58.″5, is excluded by the diaphragm.

On most nights (63) of our VV Crv campaign, we programmed the APT to make several observations of VV Crv at intervals of an hour or so, primarily to establish the out-of-eclipse light curve of the system. On the remaining 13 nights, we acquired higher-cadence monitoring observations to cover both primary and secondary eclipses as well as portions of the out-of-eclipse light curve. We describe both sets of observations below.

3.1. Out-of-eclipse Photometry

The out-of-eclipse observations were made in the following sequence, termed a group observation: *K,S,C,V,C,V,C,V,C,S,K*, where *K* is the check star (HD 109141, $V = 5.74$, $B-V = 0.38$, F3 IV-V), *C* is the comparison star (HD 110682, $V = 6.96$, $B-V = 0.31$, F0 IV), *V* is the program star (VV Crv, $V = 5.17$, $B-V = 0.43$, F5 IV), and *S* is a sky reading. Each group observation is reduced to form three bracketed $V-C$ and two unbracketed $K-C$ differential magnitudes, which are averaged together to create group means for both *B* and *V*. Group-mean differential magnitudes with internal standard deviations greater than 0.01 mag were discarded to eliminate observations taken under non-photometric conditions. The surviving group means were corrected for differential extinction with nightly extinction coefficients, transformed to the Johnson system with yearly mean transformation coefficients, and treated as single observations thereafter. T3 acquired 187 group observations during 63 non-monitoring nights of the VV Crv campaign; the resulting $V-C$ differential magnitudes in Johnson *B* and *V* are given in Table 3.

Table 3
Photometric Observations[a]

Helio. Julian Date (HJD − 2400000)	Phase	ΔV (mag)	ΔB (mag)
55992.8492	0.1831	−1.852	−1.732
55992.8837	0.1941	−1.852	−1.731
55992.9174	0.2048	−1.857	−1.729
55994.7937	0.8015	−1.844	−1.728
55994.8495	0.8192	−1.844	−1.727

Note. [a] The phases are based on parameter values listed in Table 7.

(This table is available in its entirety in machine-readable and Virtual Observatory (VO) forms in the online journal. A portion is shown here for guidance regarding its form and content.)

The standard deviations of the $K-C$ group-mean differential magnitudes are 0.0069 and 0.0083 mag for the *B* and *V* data sets, respectively, indicating that both the check and comparison stars are constant to less than 0.01 mag over the time interval of our observations. Periodogram analysis of the $K-C$ observations revealed no significant periodicity in either passband, ensuring HD 110682 is a good comparison star.

3.2. Eclipse Photometry

Higher-cadence observations were acquired on 13 nights with an extended group sequence like the one above but with 10 rather than 3 bracketed VV Crv measurements. Each of the 10 individual $V-C$ differential magnitudes, computed for each group, was treated as a single observation. Ten monitoring nights were needed to cover both eclipses; the remaining three monitoring nights were spent monitoring parts of the out-of-eclipse light curve. T3 acquired 233 monitoring groups, resulting in a total of 2330 $V-C$ differential magnitudes. All the differential magnitudes that were obtained on both the non-monitoring and monitoring nights are listed chronologically in Table 3.

4. SPECTROSCOPIC ORBIT

After acquiring a sufficient number of radial velocities to compute a preliminary orbit, we discovered that the orbital period of VV Crv is 3.145 days rather than the 1 day alias of the previous spectroscopic analyses (Sanford & Karr 1942; Massarotti et al. 2008). Searching the literature, we later learned that the *Hipparcos* team had previously determined this same 3.145 day period for the eclipses found in one of the visual binary components (Perryman & ESA 1997).

With the full spectroscopic data set in hand we adopted the period of 3.145 days and computed an orbital solution of the broad-lined primary (component 1) with BISP (Wolfe et al. 1967), a computer program that uses a slightly modified version of the Wilsing–Russell method. Because the orbit clearly

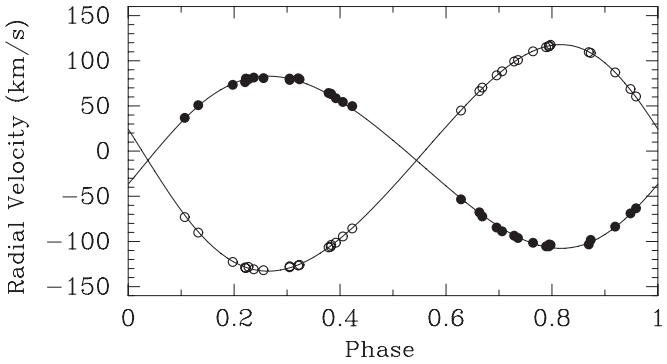

Figure 2. Fairborn Observatory radial velocities of VV Crv compared with the computed velocity curves. Primary: filled circles; secondary: open circles. Zero phase is a time of periastron passage.

Table 4
Spectroscopic Orbital Elements and Related Parameters of VV Crv[a]

Parameter	Reanalysis of Massarotti et al. (2008)	This Study
P (days)	3.144565 ± 0.000036	3.144499 ± 0.000026
T (HJD)	2454286.217 ± 0.041	2455660.383 ± 0.011
γ (km s^{-1})	−9.56 ± 0.43	−10.26 ± 0.15
K_1 (km s^{-1})	93.72 ± 0.68	95.34 ± 0.36
K_2 (km s^{-1})	124.99 ± 0.93	125.42 ± 0.19
e	0.0801 ± 0.0056	0.0861 ± 0.0016
ω_1 (deg)	253.7 ± 4.6	255.3 ± 1.3
$a_1 \sin i$ (10^6 km)	4.040 ± 0.029	4.107 ± 0.016
$a_2 \sin i$ (10^6 km)	5.387 ± 0.040	5.4031 ± 0.0081
$m_1 \sin^3 i$ ($M_\odot$)	1.929 ± 0.031	1.9695 ± 0.0084
$m_2 \sin^3 i$ ($M_\odot$)	1.447 ± 0.021	1.4971 ± 0.0102
Std error[b] (km s^{-1})	2.62	0.89

Notes.
[a] Solutions computed from spectroscopic data alone.
[b] Standard error of unit weight observation.

has a modest eccentricity despite its rather short period, the initial solution was refined with the differential corrections orbit program SB1 (Barker et al. 1967). We determined a separate orbit for the narrower lined secondary (component 2) in the same manner. Because of the much greater $v \sin i$ value of the primary, its velocities are less precise, and the variances of the orbital solutions result in weights of 0.25 and 1.0 for the primary and secondary, respectively. The center-of-mass velocities of the two solutions differ by just 0.4 km s^{-1}, and so a joint spectroscopic orbit solution of the primary and secondary was obtained. In this case we used a version of SB1 that was modified to analyze the two components simultaneously. The orbital elements and derived quantities from that spectroscopic solution are presented in Table 4. Figure 2 compares the Fairborn radial velocities with the predicted velocity curves. Zero phase is a time of periastron.

For comparison with our results, we also produced a solution of the primary and secondary velocities of Massarotti et al. (2008). To obtain the revised orbit, the velocities of the secondary were given half the weight of those of the primary. In addition, the primary and secondary velocities of JD 2453088 and JD 2454278 as well as the secondary velocity of JD 2453372, all of which had residuals larger than 10 km s^{-1}, were given zero weights in the final solution. The radial velocities compared to the computed orbital curves are shown in Figure 3, and the new orbital elements are listed in Table 4.

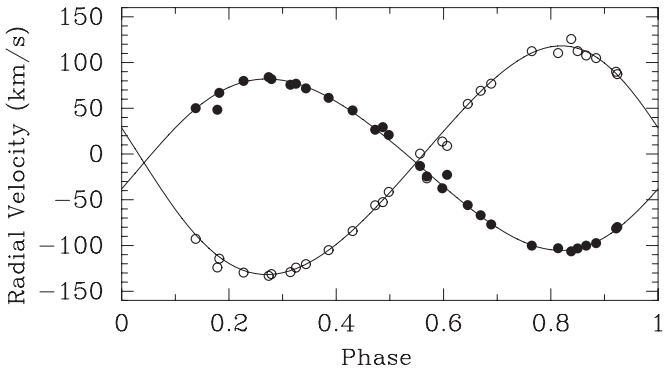

Figure 3. Radial velocities of Massarotti et al. (2008) for VV Crv compared with velocity curves that were calculated with $P = 3.14456$ days. Primary: filled circles; secondary: open circles. Zero phase is a time of periastron passage.

Table 5
Measurement Characteristics

Curve	Data Points	Normal Mag	σ[a]
Johnson V	2333	−1.858	0.0234
Johnson B	2422	−1.736	0.0134
RV_1	35	...	0.55 km s^{-1}
RV_2	35	...	0.46 km s^{-1}

Note. [a] For the light curves, in units of total light at phase 0.25.

The two sets of orbital elements are in reasonable agreement. However, our minimum masses are 2–3% larger, and the uncertainties of the elements from our velocities are about two to four times smaller. The center-of-mass velocity of our solution and the one that we determined for the velocities of Massarotti et al. (2008) differ by slightly more than their summed 1σ values. So there is currently no evidence for a close unseen tertiary companion to VV Crv. Our spectroscopic analyses clearly confirm component B of the visual pair, HR 4821, as the eclipsing system VV Crv.

5. COMBINED LIGHT AND VELOCITY SOLUTION

We next used the Wilson–Devinney (WD) program, 2003 version, to compute light and velocity solutions. Wilson & Devinney (1971) and Wilson (1979, 1990) have extensively described the physical model of the program. Now included in the program is an improved stellar atmosphere treatment (Van Hamme & Wilson 2003), based on pre-fitted Legendre functions to Kurucz (1993) atmosphere models.

The *VB* photometry and the double-lined radial velocity measurements were solved simultaneously to improve the final results (see Wilson 1979; Van Hamme & Wilson 1984, 1985, regarding this procedure). The WD program employs both curve-dependent and light-level-dependent weights. The former are correlated with the standard deviations of the observations, and these are provided in Table 5. The second type of weights are inversely proportional to the square root of the photometric light values. For the description of the limb darkening of both stars, the square-root coefficients x, y were obtained from Van Hamme (1993). The bolometric albedo (A) and the gravity-darkening (g) coefficients were obtained from Lucy (1967) for the convective-envelope case, again for both members of the system. Table 6 lists the values for all of the limb-darkening coefficients and other non-varying parameters.

The spectral type estimates of VV Crv are centered around F5 V (Cowley & Bidelman 1979; Abt 1981, 2009). The Tycho

Table 6
Non-varying WD Parameters

Parameter	Symbol	Value
Rotation/orbit ratio	F_1, F_2	1.0, 1.0
Albedo (bolo)	A_1, A_2	0.50, 0.50
Gravity darkening	g_1, g_2	0.32, 0.32
Limb darkening (bolo)	x_1, y_1	+0.116, +0.603
Limb darkening (bolo)	x_2, y_2	+0.116, +0.603
Limb darkening (V)	x_1, y_1	+0.115, +0.687
Limb darkening (V)	x_2, y_2	+0.115, +0.687
Limb darkening (B)	x_1, y_1	+0.303, +0.580
Limb darkening (B)	x_2, y_2	+0.303, +0.580

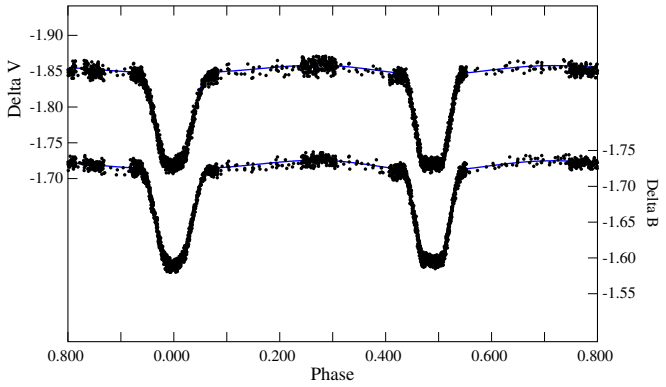

Figure 4. Differential Johnson V and B magnitudes of VV Crv plotted with the Wilson–Devinney solution curves. Zero phase is at the center of primary eclipse, and the appropriate ephemeris (from Section 6) is minimum light (HJD) = 2456045.7310 ± 0.0001 + 3.1445358 ± 0.0000097E days.
(A color version of this figure is available in the online journal.)

Double Star Catalogue (Fabricius et al. 2002) lists B_T and V_T magnitudes in the *Tycho* system for the individual A and B visual components. We converted these values to Johnson B and V magnitudes for VV Crv, which result in $V = 5.843$ and $B - V = 0.438$. As noted in Section 7, Balachandran (1990) determined an [Fe/H] abundance of 0.0, but this is likely to be a lower limit to the value. We input those values into Equation (1) of the T_e–$(B - V)$–[Fe/H] temperature scale of Alonso et al. (1996), which was derived by the Infrared Flux Method. The resulting mean temperature for the binary pair is 6487 K. Increasing [Fe/H] by 0.1 dex raises the temperature to 6543 K. For comparison, Flower (1996), who determined an empirical scale between effective temperature and $B - V$ color, gives T_e = 6541 K for $B - V = 0.44$. Thus, we adopted T_e = 6500 K for the primary, which was held constant in our solution.

With the flat light levels outside of the eclipses, it was immediately apparent that the system is detached; consequently, Mode 2 of the WD program was the appropriate mode for our analysis and solution. Due to the large separation of the components, only one reflection was employed (see Wilson 1990). Resulting quantities from the WD solution are given in Table 7. The third light parameter, due to the inclusion of the flux from VV Crv A, was computed to be 0.5092 ± 0.0020 and 0.5026 ± 0.002 in the V and B bands, respectively. The derived inclination of 88.°96 ± 0.°07 makes the orbit nearly edge-on. The eccentricity (0.0852 ± 0.0010) and mass ratio (0.765 ± 0.002) values are extremely similar to those found from the spectroscopic solution described in Section 4. Because the extensive amount of third light greatly dilutes and thus compresses the eclipse depth, the WD solution is not very sensitive to surface temperature. Although we find a formal error of just 3 K for the derived temperature of the secondary relative to that of the primary, the error in temperature for both stars is estimated to be ±200 K (Table 7). Figure 4 shows our photometric observations and the light curves computed in each bandpass from our orbital elements. Expanded views of the primary and secondary eclipses are plotted in Figures 5 and 6, respectively.

Basic properties of the system and its components are listed in Table 8. In particular, the masses are M_1 = 1.978 ± 0.010 $M_\odot$ and M_2 = 1.513 ± 0.008 $M_\odot$, and the radii are R_1 = 3.375 ± 0.010 $R_\odot$ and R_2 = 1.650 ± 0.008 $R_\odot$. The mass of the primary is that of an A2 main-sequence star, which

Table 7
Light and Velocity Curve Results[a]

Parameter	Symbol	Value
Period (days)	P	3.1445358 ± 0.0000097
Epoch of primary eclipse minimum (HJD)	T_0	2456045.7310 ± 0.0001
Eccentricity	e	0.0852 ± 0.0010
Longitude of periastron (deg)	ω_1	257.73 ± 0.16
RV semiamplitude (km s^{-1})	K_1	95.82 ± 0.05
RV semiamplitude (km s^{-1})	K_2	129.29 ± 0.05
Systemic velocity (km s^{-1})	γ	−10.14 ± 0.17
Semimajor axis ($R_\odot$)	a	13.70 ± 0.03
Inclination (deg)	i	88.47 ± 0.24
Mass ratio	M_2/M_1	0.765 ± 0.002
Surface potential	Ω_1	4.9345 ± 0.0073
Surface potential	Ω_2	7.5731 ± 0.0242
Temperature (K) (fixed)	T_1	6500[b] ± 200
Temperature (K)	T_2	6638 ± 200[c]
Luminosity ratio	$L_1/(L_1 + L_2)_V$	0.7947 ± 0.0068
Luminosity ratio	$L_1/(L_1 + L_2)_B$	0.7931 ± 0.0068

Notes.
[a] Wilson–Devinney simultaneous solution, including proximity and eclipse effects, of the light and velocity data.
[b] Adopted value, see the text.
[c] Estimated uncertainty, see the text.

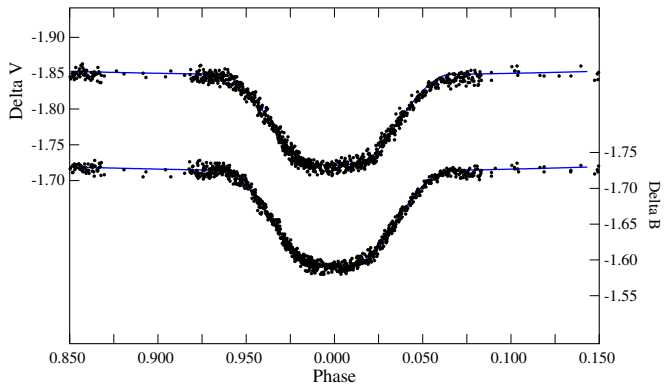

Figure 5. Expanded view of the differential Johnson V and B magnitudes of VV Crv during primary eclipse plotted with the Wilson–Devinney solution curves.

(A color version of this figure is available in the online journal.)

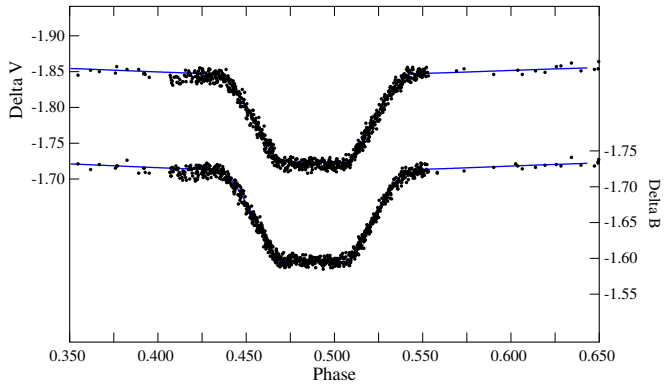

Figure 6. Expanded view of the differential Johnson V and B magnitudes of VV Crv during secondary eclipse plotted with the Wilson–Devinney solution curves.

(A color version of this figure is available in the online journal.)

has a corresponding temperature that is significantly higher than the value that we used. However, as we have seen, the mid-F spectral type classifications from the literature and the combined $B-V$ that comes from the *Tycho* observations equate to the 6500 K temperature that we adopted. The system is closer than 100 pc, so the reddening is negligible. Thus, as expected from the difference in masses, the more massive star, which dominates the spectrum and the combined light of VV Crv, has evolved to a cooler temperature. The evolutionary state of the components is examined more extensively in Section 10.

6. ECLIPSE EPHEMERIDES

For the light and velocity curve solutions described in Section 5, we used time (HJD) instead of phase as the independent variable. This allowed us to determine ephemeris parameters, reference epoch T_0 (i.e., the time of primary eclipse minimum), and period P, as part of the solution. The eclipse depths, which are substantially diluted by the light from component A of the visual binary, are very similar (Figure 4), making it somewhat difficult to identify which is the deeper, and thus primary, eclipse, but it appears to be the annular transit. Two issues must be noted about this primary eclipse. (1) While the star we have consistently designated as the primary is the more massive, larger, and brighter one, it is the cooler of the two components. Thus, primary eclipse is a transit of the hotter but smaller secondary in front of the cooler and larger primary.

Table 8
Fundamental Parameters of VV Crv

Parameter	Primary	Secondary
M ($M_\odot$)	1.978 ± 0.010	1.513 ± 0.008
R ($R_\odot$)	3.375 ± 0.010	1.650 ± 0.008
$\log g$ (cm s^{-2})	3.678 ± 0.006	4.183 ± 0.009
$M_{\rm bol}$ (mag)	1.587 ± 0.134	3.049 ± 0.134
$L/L_\odot$	18.253 ± 2.249	4.745 ± 0.583
V (mag)	6.099 ± 0.073	7.536 ± 0.073
B (mag)	6.541 ± 0.072	7.959 ± 0.072
Spectral type	F5 dwarf	F5 dwarf
$v_{\rm rot}$ (km s^{-1})	81 ± 3	24 ± 2

(2) Due to the eccentric orbit and the position angles of the system, the computed zero phase by the WD program does not occur at the center of primary eclipse. The superior conjunction phase (i.e., center of primary eclipse) is computed at 0.006145, the inferior conjunction is at phase 0.494578, and the periastron phase is 0.465926. We have shifted the time of mid-primary eclipse to phase 0.0 and accordingly adjusted the T_0 value. Our new eclipse ephemeris is

$$\text{minimum light (HJD)} = 2456045.7310 \pm 0.0001 + 3.1445358 \pm 0.0000097E \text{ days},$$

where E represents an integer number of cycles. Correspondingly, the center of secondary eclipse is now at phase 0.488433 and periastron is at 0.459781. The time of secondary minimum occurs at

$$\text{minimum light (HJD)} = 2456047.2669 \pm 0.0001 + 3.1445358 \pm 0.0000097E \text{ days}.$$

Given the limited timespan of our data set, we made no attempt with the WD program to search for any period change.

7. SPECTRAL TYPES AND SPECTROSCOPIC MAGNITUDE DIFFERENCE

Our examination of the spectral types of VV Crv followed the general procedure used by Strassmeier & Fekel (1990). They found several temperature-sensitive and luminosity-sensitive line ratios in the 6430–6465 Å region. In addition to those line ratios, they used the general appearance of the spectrum as spectral-type criteria. Unfortunately, for F dwarfs and subgiants their identified line ratios have little sensitivity to luminosity.

The close visual components A and B have similar mid-F spectral types (Cowley & Bidelman 1979; Abt 1981, 2009). In particular, Cowley & Bidelman (1979) classified VV Crv as F3 Vn, while Abt (1981) first gave it a spectral type of F5 V and later a type of F7 V (Abt 2009). Thus, we compared a KPNO spectrum of VV Crv with those of several slowly rotating F dwarfs taken from the lists of Keenan & McNeil (1989) and Fekel (1997). We acquired the spectra of our various comparison stars at KPNO with the same telescope, spectrograph, and detector as our spectrum of VV Crv. We attempted to reproduce the spectrum of VV Crv in the 6430 Å region by using a computer program developed by Huenemoerder & Barden (1984) and Barden (1985). Trial combinations of the reference-star spectra were obtained by applying rotational broadening to the lines, shifting the spectra to obtain the observed velocity separation of VV Crv, and assigning appropriate weights.

The best fit to the spectrum of VV Crv occurred when we adopted HR 7469 (F4 V, Slettebak 1955; [Fe/H] = 0.01, Taylor

2005) for both the primary and secondary, although some of the comparison star lines were not strong enough. A fit with HR 3775 (F6 IV, Johnson & Morgan 1953; [Fe/H] = −0.17, Taylor 2005) for both components produced a similar result. Thus we adopt an F5 spectral class for both components and conclude that the components are metal rich relative to the Sun. The absolute magnitudes indicate that the more massive primary is approaching the end of its main-sequence lifetime, while the secondary, which has a significantly lower mass, is still clearly on the main sequence.

Balachandran (1990) determined an iron abundance for VV Crv from spectrum synthesis of a high-resolution spectrum, finding [Fe/H] = 0.0, relative to the Sun. However, that result did not account for the dilution of the primary lines that results from the presence of the spectroscopic binary secondary. Thus, the lines of the primary would be intrinsically stronger and result in an abundance that is greater than the solar value.

From our KPNO spectrum, the resulting continuum intensity ratio I_2/I_1 is 0.1904. Because of the similarity of the spectral classes, we adopt this value as the luminosity ratio, which corresponds to a magnitude difference in the 6430 Å region of 1.8 mag with an estimated uncertainty of 0.3 mag.

8. MAGNITUDES AND DISTANCE

As noted earlier, from our conversion of the Tycho Double Star Catalogue magnitudes for VV Crv we determined $V = 5.843 \pm 0.010$ and $B - V = 0.438 \pm 0.010$ for the maximum amount of combined light outside eclipse. From the WD solution we obtain the bolometric magnitudes and the individual luminosity ratios as a function of phase. The bolometric correction for a 6500 K main-sequence star is +0.006 mag (Flower 1996), which results in $M_V = 1.581 \pm 0.134$. The luminosity ratio of the two components in the V bandpass at phase 0.250 is 0.266, producing a magnitude difference of 1.437. Thus, the primary is 0.256 mag fainter than the combined V mag and so has $V = 6.099 \pm 0.073$ mag. From the absolute and apparent magnitudes, the computed distance is 80.1 ± 5.6 pc. The original *Hipparcos* parallax was $0\farcs01172 \pm 0\farcs00190$ (Perryman & ESA 1997), which was revised to $0\farcs01267 \pm 0\farcs00097$ by van Leeuwen (2007). The corresponding distances are 85.3 ± 13.8 pc and 78.9 ± 6.0 pc, respectively. Thus, the revised *Hipparcos* distance differs from our slightly more precise value by just 1.2 pc. These and related properties are summarized in Table 8.

9. CIRCULARIZATION AND SYNCHRONIZATION

Exploring two different mechanisms, Zahn (1977) and Tassoul & Tassoul (1992) computed orbital circularization and rotational synchronization time scales. While the results of those analyses disagree significantly on absolute time scales, the two mechanisms both predict that rotational synchronization should occur before orbital circularization. Duquennoy & Mayor (1991) examined the multiplicity of solar-type stars in the solar neighborhood and concluded that the vast majority of systems with periods $\leqslant$10 days have circular orbits. Solar-type stars with longer orbital periods generally have eccentric orbits. Of course, although both components of VV Crv are currently mid-F stars, the primary began its main-sequence life as an early-A star. Matthews & Mathieu (1992) surveyed known A-star spectroscopic binaries and found that circular or nearly circular orbits occur for all systems with orbital periods $\lesssim$3 days. VV Crv has a period of 3.145 days, slightly greater than the 3 day limit. Thus, in the context of the A-star results, the system would appear to be a bit unusual because of its non-zero eccentricity of 0.085.

VV Crv, however, is not an isolated short-period binary but part of a multiple system. Building on their previous work with triple systems, Eggleton & Kiseleva-Eggleton (2006) explored a combination of Kozai cycles (Kozai 1962) and tidal friction as a mechanism for altering the characteristics of the inner orbits in triple systems. The former are cyclic changes in a short-period orbit such as the periodic modulation of its eccentricity, caused by tertiary companion perturbations. If at some point the separation of the short-period pair becomes sufficiently small, then tidal friction drains energy from the inner orbit and eventually circularizes it. Thus, Eggleton & Kiseleva-Eggleton (2006) argued that the combination of these two processes, referred to as Kozai cycles with tidal friction (KCTF), could well result in many short-period binaries. This prediction appears to be confirmed by the work of Tokovinin et al. (2006), who surveyed 165 solar-type spectroscopic binaries and found that 96% of such binaries with periods less than 3 days had tertiary companions. They also found a significant difference in the period distribution of spectroscopic binaries with and without additional companions and concluded that a tertiary companion decreases the orbital period of a spectroscopic binary. Theoretical work by Fabrycky & Tremaine (2007) showed that in a triple system the KCTF mechanism produces inner binaries with periods of up to 10 days from binaries that began with periods ranging up to 100,000 days. They also reported that the peak of the final short-period distribution is 3 days.

As we have noted, VV Crv is part of at least a quintuple and perhaps a sextuple system. With an orbital period of 3.145 days, its orbit fits very well into the observational and theoretical framework reviewed above. This argues that the system has been perturbed by a long-period companion. VV Crv is part of a common proper motion pair, so a companion to VV Crv is clearly evident. The current projected separation from component A is 5″.2. Such an angular separation translates into a projected linear separation of 416 AU, which results in an estimated period of 3455 yr from Kepler's third law. Tokovinin (2008) pointed out that for many triple systems the outer companion is too far away to produce KCTF migration; however, their inner periods are statistically shorter than isolated short-period binaries. So, either such distant companions still produce significant effects over time or perhaps such triple systems have as yet undiscovered intermediate companions. The former situation would not seem to be the case for VV Crv. Adopting the projected linear separation as the semimajor axis of the common proper motion pair, from Kisseleva-Eggleton & Eggleton (2010) the estimated Kozai cycle period is ∼1 trillion yr. On the other hand, we note that our observations provide no evidence of a substantially closer additional companion to VV Crv.

In Section 10 (below) we determine an age of 1.2 Gyr for VV Crv. For a star with a convective outer atmosphere, Equation (6.2) of Zahn (1977) produces a circularization time of 0.5 Gyr for the orbit of VV Crv, while the circularization time from the theory of Tassoul (Tassoul & Tassoul 1995) is even shorter. Thus, both estimates would indicate that the orbit of VV Crv should be circularized. However, we note that the primary of VV Crv was an A star with a radiative envelope for most of its lifetime, and the convective envelope of the secondary is very thin. Zahn (1977) noted that the time scale for circularization of a star with a radiative envelope is orders

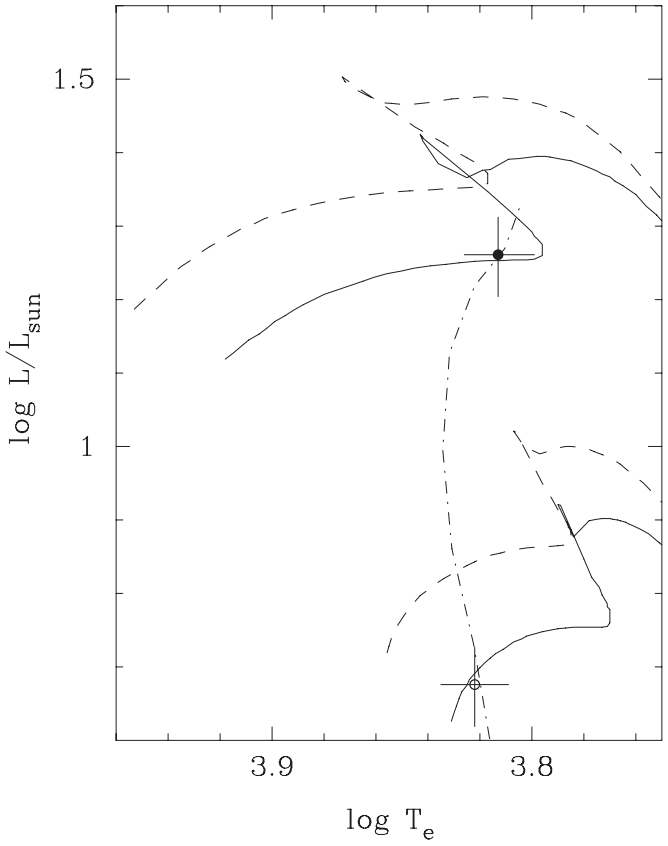

Figure 7. Positions of the two components of VV Crv (primary: filled circle; secondary: open circle) with their uncertainties in a theoretical H-R diagram compared with the Yonsei–Yale evolutionary tracks (dashed lines for [Fe/H] = 0.0, solid lines for [Fe/H] = 0.3). The dot–dashed line is the 1.2 Gyr isochrone.

of magnitude larger than for a star with a convective envelope. Thus, even if the common proper motion companion is too distant to have a significant effect, it may not be surprising that the orbit has not yet circularized despite its rather short period.

From the work of Hut (1981) it is known that in an eccentric orbit the rotational angular velocity of a star will tend to synchronize with that of the orbital motion at periastron. This situation is called pseudosynchronous rotation. We use Equation (42) of Hut (1981) to compute a pseudosynchronous period of 3.01 days for VV Crv. That period and the radii from the light curve solution (Table 8) result in pseudosynchronous rotational velocities of 56.8 and 27.7 km s^{-1} for the primary and secondary, respectively.

For comparison with the above pseudosynchronous values, we have determined observed rotational velocities. From the rotational broadening fits to the lines of 30 Fairborn spectra we have measured projected rotational velocities of 81 ± 3 and 24 ± 2 km s^{-1} for the more massive primary and less massive secondary, respectively. If, as is generally assumed, the orbital and rotational axes are parallel, then the two inclinations are equal. In the case of VV Crv, the orbital inclination is nearly 90° so we just adopt our v sin i values of the two stars as their rotational velocities. The primary is rotating about 40% faster than its pseudosynchronous value, while the secondary is rotating nearly 15% slower than its pseudosynchronous rate.

Since the primary began life on the main sequence as an early-A star, its original rotational velocity was probably significantly larger than its current value. For example, Table B1 of Gray (1992) gives a mean v sin i value of ∼140 km s^{-1} for a 2 $M_\odot$ early-A star. Thus, the primary is likely spinning down to its pseudosynchronous velocity from a much larger value and for much of its life has had a radiative envelope. Again, Zahn (1977) points out that the synchronization time scale for a star with a radiative envelope is orders of magnitude larger than for a star with a convective envelope. For the secondary, which is much more slowly rotating, the observed rotational velocity is within 2σ of the pseudosynchronous value, so it is not far off.

10. EVOLUTIONARY STATUS

In Figure 7 we show the positions of the primary and secondary of VV Crv in a theoretical H-R diagram. Also plotted in the log T_e–log $L/L_\odot$ plane are stellar evolutionary tracks from the Yonsei–Yale series (Yi et al. 2001; Demarque et al. 2004) for the specific masses that we determined for the primary and secondary. There are two tracks for each mass, one with metal abundance $Z = 0.018$, corresponding to [Fe/H] = 0.0 or solar metallicity, and the other for $Z = 0.034$, corresponding to a metal rich composition, [Fe/H] = 0.3. Our result from the spectrum comparison analysis that the components of VV Crv are slightly metal rich is confirmed by the near agreement of the primary and secondary components with the metal-rich $Z = 0.034$ tracks. Within the error bars, both components have an age of 1.2 ± 0.1 Gyr. The more massive primary, which was originally an early-A star, is near the end of its main-sequence lifetime, and in about 0.15 Gyr it will begin to evolve across the Hertzsprung gap. The less massive secondary remains well ensconced on the main sequence. Thus, although the two components differ in temperature by just 138 K, the significant mass difference has caused them to be at rather different stages in their main-sequence evolution.

11. SUMMARY

With the WD program we have analyzed new Johnson B and V photometric observations and radial velocities of the mid-F eclipsing binary VV Crv. The combined solution results in an orbital period of 3.1445358±0.0000097 days and a significantly non-zero eccentricity of 0.085 ± 0.001. Although the eclipses of VV Crv are total, its close visual companion results in a significant third-light contribution that substantially reduces the depth of the eclipse light curve. Despite this complication, the masses and radii of the primary and secondary, M_1 = 1.978 ± 0.010 $M_\odot$ and M_2 = 1.513 ± 0.008 $M_\odot$, and R_1 = 3.375 ± 0.010 $R_\odot$ and R_2 = 1.650 ± 0.008 $R_\odot$, respectively, are determined to a precision of 0.5%. We compute a distance to the system of 80.1 ± 5.6 pc, which is in good agreement with the revised *Hipparcos* value of 78.9 ± 6.0 pc (van Leeuwen 2007). When compared with the predicted pseudosynchronous rotational velocities, the primary is rotating more than 40% faster while the secondary is spinning nearly 15% slower. While the effective temperature difference of the components is less than 150 K, the very significant mass difference positions the stars at somewhat different places in an H-R diagram. The primary is nearly finished with its main-sequence life, but the secondary is just roughly one-third of the way toward that end. A comparison with metal-rich evolutionary tracks, $Z = 0.034$, indicates that the components have an age of 1.2 ± 0.1 Gyr.

We acknowledge NSF support through grant 1039522 of the Major Research Instrumentation Program. In addition, astronomy at Tennessee State University is supported by the state of Tennessee through its Centers of Excellence programs.

We thank Walter Van Hamme for advice regarding the WD program and for computing the error bars of the parameters of the final solution. This research made use of the SIMBAD database, operated at CDS, Strasbourg, France.

REFERENCES

Abt, H. A. 1981, ApJS, 45, 437
Abt, H. A. 2009, ApJS, 180, 117
Alonso, A., Arribas, S., & Martínez-Roger, C. 1996, A&A, 313, 873
Armstrong, J. T., Hummel, C. A., Quirrenbach, A., et al. 1992, AJ, 104, 2217
Balachandran, S. 1990, ApJ, 354, 310
Barden, S. C. 1985, ApJ, 295, 162
Barker, E. S., Evans, D. S., & Laing, J. D. 1967, RGOB, 130, 355
Boden, A. F., Torres, G., & Hummel, C. A. 2005, ApJ, 627, 464
Cowley, A. P., & Bidelman, W. P. 1979, PASP, 91, 83
Demarque, P., Woo, J.-H., Kim, Y.-C., & Yi, S. K. 2004, ApJS, 155, 667
Duquennoy, A., & Mayor, M. 1991, A&A, 248, 485
Eaton, J. A., Henry, G. W., & Fekel, F. C. 2003, in The Future of Small Telescopes in the New Millennium, Vol. II, The Telescopes We Use, ed. T. D. Oswalt (Dordrecht: Kluwer), 189
Eaton, J. A., & Williamson, M. H. 2007, PASP, 119, 886
Eggleton, P. P., & Kiseleva-Eggleton, L. 2006, Ap&SS, 304, 75
Fabricius, C., Hog, E., Makarov, V. V., et al. 2002, A&A, 384, 180
Fabrycky, D., & Tremaine, S. 2007, ApJ, 669, 1298
Fekel, F. C. 1997, PASP, 109, 514
Fekel, F. C., & Griffin, R. F. 2011, Obs, 131, 283
Fekel, F. C., Rajabi, S., Muterspaugh, M. W., & Williamson, M. H. 2013, AJ, 145, 111
Fekel, F. C., & Tomkin, J. 2004, AN, 325, 649
Fekel, F. C., Tomkin, J., & Williamson, M. H. 2009, AJ, 137, 3900
Flower, P. J. 1996, ApJ, 469, 355
Gray, D. F. 1992, The Observation and Analysis of Stellar Photospheres (Cambridge: Cambridge Univ. Press)
Halbwachs, J. L., Mayor, M., Udry, S., & Arenou, F. 2003, A&A, 397, 159
Henry, G. W. 1995, in ASP Conf. Ser. 79, Robotic Telescopes: Current Capabilities, Present Developments, and Future Prospects for Automated Astronomy, ed. G. W. Henry & J. A. Eaton (San Francisco, CA: ASP), 44
Henry, G. W. 1999, PASP, 111, 845
Huenemoerder, D. P., & Barden, S. C. 1984, BAAS, 16, 510
Hut, P. 1981, A&A, 99, 126
Johnson, H. L., & Morgan, W. W. 1953, ApJ, 117, 313
Johnson, J. A., Clanton, C., Howard, A. W., et al. 2011, ApJS, 197, 26
Kazarovets, V., Samus, N. N., Durlevich, O. V., et al. 1999, IBVS, 4659, 1
Keenan, P. C., & McNeil, R. C. 1989, ApJS, 71, 245
Kisseleva-Eggleton, L., & Eggleton, P. P. 2010, in ASP Conf. Ser. 435, Binaries—Keys to Comprehension of the Universe, ed. A. Prsa & M. Zejda (San Francisco, CA: ASP), 169
Kozai, Y. 1962, AJ, 67, 591
Kurucz, R. L. 1993, in Light Curve Modeling of Eclipsing Binary Stars, ed. E. F. Milone (New York: Springer), 93
Lucy, L. B. 1967, ZA, 65, 89
Mason, B. D., Hartkopf, W. I., Wycoff, G. L., & Wieder, G. 2007, AJ, 134, 1671
Massarotti, A., Latham, D. W., Stefanik, R. P., & Fogel, J. 2008, AJ, 135, 209
Matthews, L. D., & Mathieu, R. D. 1992, in ASP Conf. Ser. 32, Complimentary Approaches to Double and Multiple Star Research, IAU Colloquium 135, ed. H. A. McAlister & W. I. Hartkopf (San Francisco, CA: ASP), 244
Mayor, M., & Mazeh, T. 1987, A&A, 171, 157
Perryman, M. A. C., & ESA 1997, The Hipparcos and Tycho Catalogues (ESA SP-1200; Noordwijk: ESA)
Pourbaix, D., Tokovinin, A. A., Batten, A. H., et al. 2004, A&A, 424, 727
Sanford, R. F., & Karr, E. 1942, ApJ, 96, 214
Scarfe, C. D. 2010, Obs, 130, 214
Shajn, G., & Albitzky, V. 1932, MNRAS, 92, 771
Sinachopoulos, D. 1993, A&AS, 99, 11
Slettebak, A. 1955, ApJ, 121, 653
Strassmeier, K. G., & Fekel, F. C. 1990, A&A, 230, 389
Tassoul, J.-L., & Tassoul, M. 1992, ApJ, 395, 259
Tassoul, J.-L., & Tassoul, M. 1995, FCPh, 16, 377
Taylor, B. J. 2005, ApJS, 161, 444
Tokovinin, A. 2008, MNRAS, 389, 925
Tokovinin, A., Thomas, S., Sterzik, M., & Udry, S. 2006, A&A, 450, 681
Van Hamme, W. 1993, AJ, 106, 2096
Van Hamme, W., & Wilson, R. E. 1984, A&A, 141, 1
Van Hamme, W., & Wilson, R. E. 1985, Ap&SS, 110, 169
Van Hamme, W., & Wilson, R. E. 2003, in ASP Conf. Ser. 298, GAIA Spectroscopy, Science and Technology, ed. U. Munari (San Francisco, CA: ASP), 323
Van Leeuwen, F. 2007, *Hipparcos*, The New Reduction of the Raw Data (Astrophysics and Space Science Library, Vol. 350; Berlin: Springer)
Wilson, R. E. 1979, ApJ, 234, 1054
Wilson, R. E. 1990, ApJ, 356, 613
Wilson, R. E., & Devinney, E. J. 1971, ApJ, 166, 605
Wolfe, R. H., Horak, H. G., & Storer, N. W. 1967, in Modern Astrophysics, ed. M. Hack (New York: Gordon & Breach), 251
Yi, S. K., Demarque, P., Kim, Y.-C., et al. 2001, ApJS, 136, 417
Zahn, J.-P. 1977, A&A, 57, 383